Porous - Hydroxyapatite Nanoflakes by Ascorbic Acid Additive in wet- chemical Combustion Synthesis

P.Varun Prasath , B. Subha, R. Abinaya , R. J. Kavitha, K. Ravichandran*

[1]Department of Analytical Chemistry, University of Madras, Guindy Campus, Chennai, India.

**Corresponding author mail : raavees@gmail.com*

Abstract— **Porous Hydroxyapatite (HAP, $Ca_{10}(PO_4)_6(OH)_2$ possessing bioactivity, biocompatibility, solubility and adsorption is highly useful as a biomaterial in various applications . Pure HAP nanoparticles were synthesized at moderate temperatures by wet chemical synthesis and subjecting it to combustion method with a organic fuel (ascorbic acid). The X-ray diffractometry (XRD) and Fourier transform Infrared (FTIR) spectrometry were used to characterize these nanoparticles,and the morphological features of these particles were observed by Scanning electron microscopy (SEM).**

Introduction

The similarity in composition and structure of Hydroxyapatite (HAP) to that of nature bone and tooth make it as a good biocompatible and bioactive material. The applications include bone substitution, drug delivery agent and dental fillers [1−5]. It is well known that the applications of HAP depend on its properties, which are influenced greatly by the size and morphology of particles. The HAP whiskers could act as reinforcement phase to improve the mechanical properties and reliability of HAP ceramics [6]. HAP can be synthesized by many methods including conventional routes such as solid-state reactions and wet chemical routes based on precipitation at low temperature. Therefore, the combination of these solid satate and wet chemical precipitation process with suitable additives as fuel may provide an economical and manipulable method to prepare HAP with desirable characteristics.

Soluble collagen and gelatin, the main structural protein in vertebrates, were used to mimic the composition and structure of natural bone [7−9]. Nanocrystalline HAP with controlled-morphology was prepared by this biomimetic method, but a practical problem on such a kind of HAP was its high cost [10]. Several common organic modifiers, such as trisodium citrate, tween 20, polyethylene glycol (MW 600) [11], cetyltrimethylamonium bromide (CTAB) [7, 12], ethylenediamine tetraacetic acid (EDTA) [13−14], polyvinyl alcohol (PVA) and poly (amido-amine) (PAMAM) dendrimers[14] were used in the morphology-controlled synthesis of HAP resulting in nanofiber [13], rod-like [7] and ellipsoid-like [14] morphologies

In this work, an economical and manipulable method is atempted to control the size of HAP nanoparticles by the addition of additive Ascorbic acid.

I. MATERIALS AND METHODS

A. Chemicals and Materials

Calcium nitrate ($Ca(NO_3)_2$).$4H_2O$ and diammonium hydrogen phosphate ($(NH_4)_2HPO_4$) were used as the raw agents, and ammonium hydroxide ($NH_3 \cdot H_2O$, 30%) was used to adjust pH value. The Ascorbic acid was employed as the additives. All reagents used were analytical grade.

B. Synthesis of HAP

A 50mL solution of Calcium Nitrate (1M) was adjusted to pH=11 with concentrated ammonia solution, to that 1M of additive solution is mixing thoroughly. A 50 mL solution of Ammonium dihydrogen phosphate (0.6M) was brought to pH=11 with aqueous ammonia. The calcium nitrate solution was vigorously stirred at room temperature. The pH value of solution then adjusted to 11 by adding 1:1 NH4OH. The phosphate solution was added drop wise for two hours with vigorous stirring to produce a white semi gelatinous precipitate which was stirred for 24hours. The changes in the pH of the reaction system during HAP synthesis were maintained with aqueous ammonia at pH=11 using precipitated HAP and the addition is continued until pH meter.

Addition of Con. HNO_3 to the sample which dissolves at the pH adjusted to 1. Resultant solution is stirred until the formation of transparent gel at the temperature of 80°C. Gel formed is kept in a preheated muffle furnace at 250°C and it undergoes combustion with a bright flame. Black colored precursor obtained is sintered at 800°C for 2 hours, which results in a pure white nanocrystalline hydroxyapatite.

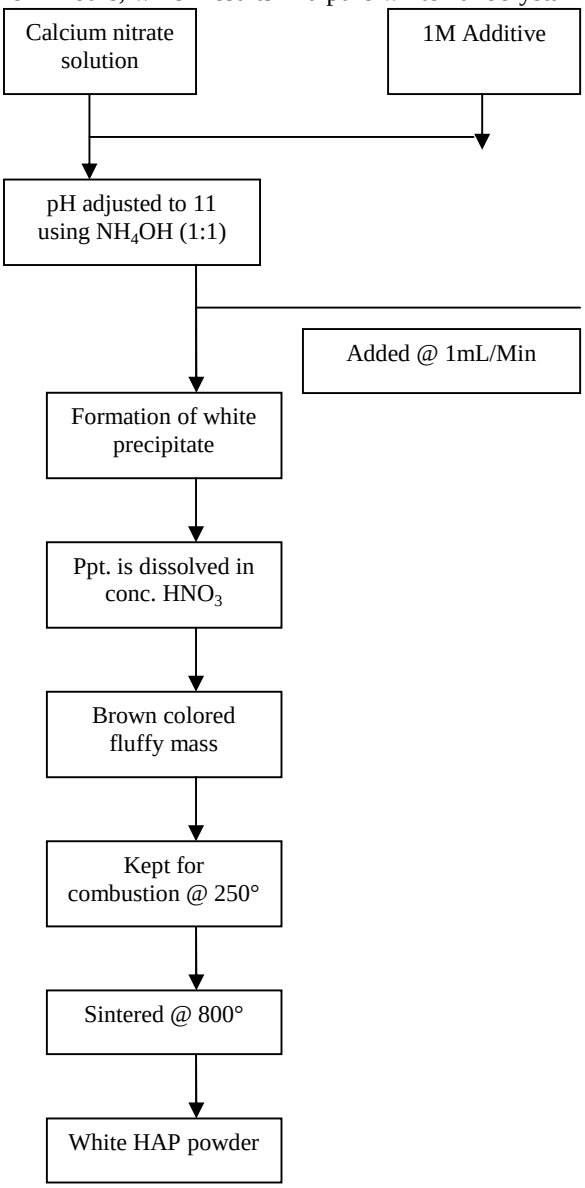

*C. **Characterization***

A Schimadzu FT-IR 8300 series was used for recording IR spectrum for HAp an polymer composites. The samples were scanned at the range of 4000 to 400 cm-1 by KBr pellet technique. Phase analysis was performed using BRUKER D8 advance X-ray Diffractometer (XRD).Synthesized HAp powder were characterized using XRD to determine the fraction of crystallinity, crystallite size, specific surface area. The crystallite size of the sample was calculated from the Scherrer's equation [12],

$$Xs = 0.9\lambda / \beta\cos\theta$$

Where, λ is the wavelength CuKα radiation source (λ=1.54A°)
β is the full width half maximum,
θ is the angle of diffraction
The morphology of the sample was investigated using FESEM (HITACHI SU6600)

II. RESULTS AND DISCUSSIONS

A. FTIR analysis

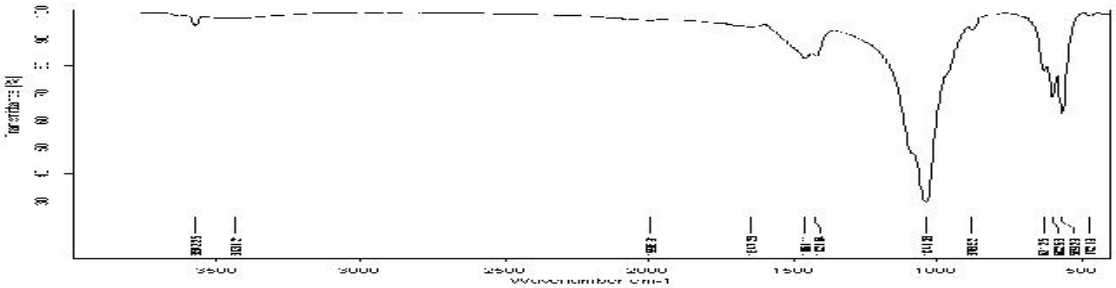

FIG.3.1.REPRESENTS FTIR ANALYSIS OF SINTERED HAP

Fig.1 shows FTIR spectra of sample synthesized with additive ascorbic acid. The bands at 565.39, 603.71, 962.52 cm^{-1} are derived from the phosphate modes. The strong bands at 1035.67 and 1099.37 cm^{-1} are assigned to the P—O stretching vibration of PO_4^{3-}, standing for phosphate mode. The absorption band at 1632.34 cm^{-1} reflects H_2O bending mode. The band at 3442.18 cm^{-1} may come from lattice H_2O since this band lies in the range of 3550−3200 cm^{-1}. The stretching, vibration and bending modes of the OH^- group appeared at 3570.41 and 633.91 cm^{-1}, respectively. The weak absorption band at 1384.80 cm^{-1} stands for carbonate that might come from the atmospheric carbon dioxide while handling the powders.

B. Raman Analysis:

The Raman spectrum of the sample is as shown in (Fig. 2). The band at 954 cm^{-1} is assigned to the strongest P–O stretching mode of HAp. The bands observed in the region 1,000–1,150 cm^{-1} are attributed to P–O stretching mode. The bands at 421, 437 and 573 cm^{-1} are assigned to O–P–O doubly degenerated bending mode. The splitting of peaks at (1028, 1044, and 1089 cm^{-1}) are suggested the co-existence of HAp and α & β-TCP [15].

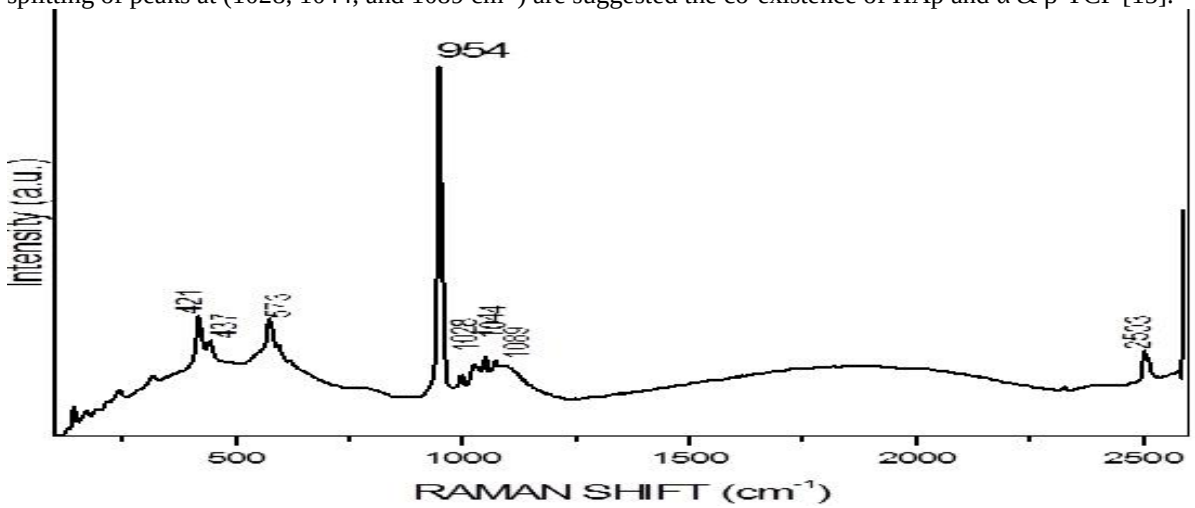

Fig..2. REPRESENTS THE RAMAN ANALYSIS OF THE SAMPLES

C. X-Ray Diffraction:

The XRD diffraction pattern is in a good agreement with the standard HAP $(Ca_{10}(PO_4)_6(OH)_2$, JCPDS No.9−0432). No characteristic peaks of impurities in (Fig.3), such as calcium hydroxide and calcium phosphates, were observed, which means that pure HAP phase was prepared under the present experimental conditions. The diffraction pattern of the sample shows that the sample is in hexagonal phase with space group of $p6_3m$. The crystallite size of the sample was calculated using Debye Scherrer formula.

The mean grain size of HAP powder was determined by Debye-Scherrer formula.

$$D = \frac{0.9\,\lambda}{\beta \cos\theta}$$

Where D represents mean grain size, B stands for full width at half maximum of the peak, λ is the diffraction angle. (Fig -3) shows a sharp and well defined XRD pattern for hydroxyapatite, it is found that HAP is the main phase and the sample got good crystallinity. Absence of peak at 37.36 indicates the absence of free CaO.

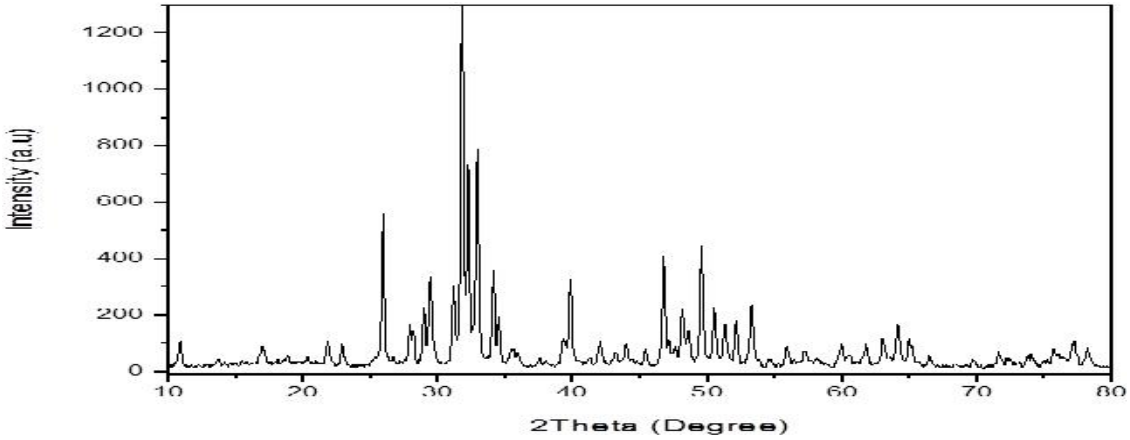

. **FIG:.3.X-RAY DIFFRACTION ANALYSIS:**

D. **FESEM Morphology Studies**

The FESEM observations of the sample (Fig. 4) revealed particles composed of irregular shape and with well defined porous morphology with typical width of 500 nm. The FESEM data revealed that the morphology of the sample is in the form of porous dense flakes .

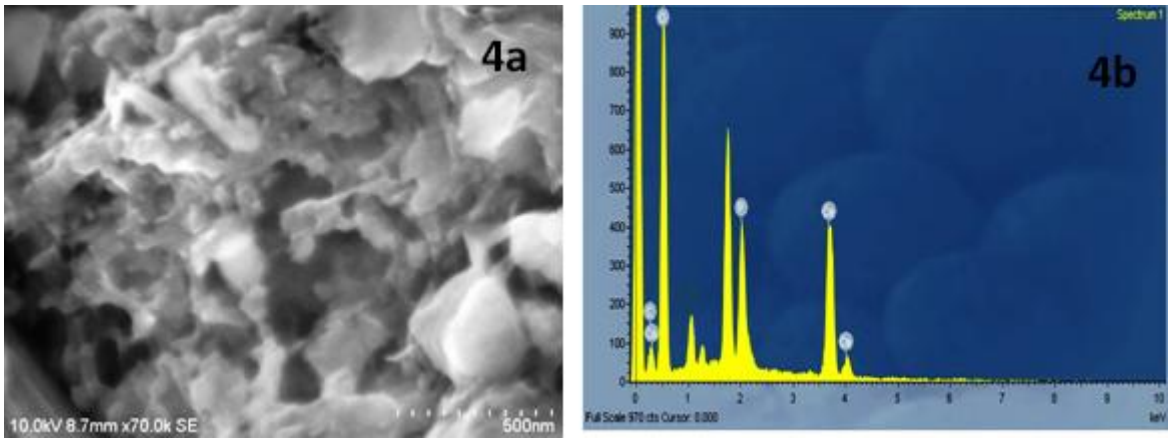

FIG. 4. FESEM AND EDX IMAGES

E. **Energy-dispersive X-ray spectroscopy (EDX)** on the sample showed that the average molar ratios of the elemental calcium and phosphorous (Ca/P) is 1.66 ; this value is in good agreement with the stoichiometric value for HAP (Ca/P = 1.67) as well as with the initial molar ratio under wet chemical precipitation method of synthesis. EDX spectrum has been shown in (Fig 4.b)

Conclusion

In this present work, synthesis of porous hydroxyapatite has been achieved by the precipitation followed by combustion synthesis. The functional groups corresponding to HAP established by FTIR and RAMAN techniques. The XRD analysis showed a phase pure HAP. The morphological study of the sample shows that the sample are in porous flakes form, this is due the dissolution of the sample by Con.HNO_3 and repeating combustion synthesis with the dissolved solution. The Ca/P ratio in the sample is matched with the theoretical HAP value 1.67 using EDX.

ACKNOWLEDGEMENT

We acknowledge the NCNSNT, University of Madras for providing the characterization facilities and University of Madras for the financial assistance as URF

REFERENCE

[1] Jevtic M, Mitric M, Skapin S, Jancar B, Ignjatovic N,Uskokovic D. Crystal structure of hydroxyapatite nanorods synthesized by sonochemical homogeneous precipitation[J]. Crystal Growth and Design, 2008, 8(7):2217−2222.

[2] Zou Jian-peng, Ruan Jian-ming, Huang Bai-yun, Liu Jian-ben,Zhou Xiao-xia. Physico-chemical properties and microstructure of hydroxyapatite 2316L stainless steel biomaterials [J]. Journal of
Central South University of Technology, 2004, 11(2): 113−118.

[3] Matsumoto T, Okazaki M, Inoue M, Yamaguchi S,Kusunose T, Toyonaga T, Hamada Y, Takahashi J. Hydroxyapatite particles as a controlled release carrier of protein[J].Biomaterials, 2004, 25:3807−3812.

[4] Zhu Shai-hong, Huang Bai-yun, Zhou Ke-chao, Huang Su-ping, Liu Fang, Li Yi-ming. Hydroxyapatite nanoparticles as a novel gene carrier[J]. Journal of Nanoparticle Research, 2004,6:307−311.

[5] Ioku K, Yamauchi S, Fujimori H, Goto S, Yoshimura M. Hydrothermal preparation of fibrous apatite and apatite sheet[J]. Solid State Ionics, 2002, 151: 147−150.

[6] Park Y M, Ryu S C, Yoon S Y, Stevens R, Park HC,Preparation of whisker-shaped hydroxyapatite β-tricalcium phosphate composite[J]. Materials Chemistry and Physics, 2008, 109: 440−447.

[7] Chang M C, Ikoma T, Kikuchi M, Tanaka J. Crosslinkage of hydroxyapatite/collagen nanocomposite using glutaraldehyde[J].Journal of Materials Science: Materials in Medicine, 2002, 13:
993−997.

[8] Chang M C, Koc C, Douglas W H. Preparation of hydroxyapatite-gelatin nanocomposite[J]. Biomaterials, 2003, 24: 2853−2862.

[9] Zhai Y, Cuif Z. Recombinant human-like collagen directed growth of hydroxyapatite nanocrystals[J]. Journal of Crystal Growth,
2006, 291: 202−206.

[10] Wang A L, Yin H B, Liu D, Wu H X, Wada Y J, Ren M, Xu Y Q, Jiang T S, Cheng X N. Effects of organic modifiers on the size-controlled synthesis of hydroxyapatite nanorods[J]. Applied
Surface Science, 2007, 253: 3311−3316.

[11] Liu Ying-kai, Wang Wen-zhong, Zhan Yong-jie, Zheng Chang-lin, Wang Guang-hou. A simple route to hydroxyapatite nanofibers[J]. Materials Letters, 2002, 56: 496−501.

[12] Kandori K, Horigami N, Yasukawa A, ishikawat. Texture and formation mechanism of fibrous calcium hydroxyapatite particles prepared by decomposition of calcium−EDTA chelates [J].
Journal of the American Ceramic Society, 1997, 80: 1157−1164.

[13] Arce H, Montero M L, Saenz A, Castanov M. Effect of pH and temperature on the formation of hydroxyapatite at low temperatures by decomposition of a Ca–EDTA complex[J]. Polyhedron, 2004, 23: 1897−1901.

[14] Yan Si-jia, Zhou Zhuo-hua, Zhang Fan, Yang Shi-ping, Yang Lian-zhun, Yu Xi-bin. Effect of anionic PAMAM with amido groups starburst dendrimers on the crystallization of Ca10(PO4)6(OH)2 by hydrothermal method[J]. Materials Chemistryand Physics, 2006, 99: 164−169.

[15] Hydrothermal synthesis of porous triphasic hydroxyapatite/(α and β) tricalcium phosphateR. Vani ,E. K. Girija,K. Elayaraja ,S. Prakash Parthiban ,R. Kesavamoorthy ,S. Narayana Kalkura J Mater Sci: Mater Med (2009) 20:S43–S48